Chiral Recognition Among Trisdiimine−Metal Complexes, 7[‡]

Racemic Compound Formation *versus* Conglomerate Formation with $[M(bpy)_3](PF_6)_2$ (M = Ni, Zn, Ru); Lattice Energy Minimisations and Implications for Structure Prediction

Josef Breu,*[a] Holger Domel,[a] and Per-Ola Norrby[b]

Keywords: Molecular recognition / Chiral recognition / Conglomerate crystallisation / Crystal structure prediction / Polymorphism

Polymorphism observed with $[M(bpy)_3](PF_6)_2$ (M = Ru, Ni, Zn) offers a unique opportunity to study the impact of different intermolecular packing motifs on lattice energies. Additionally, it allows us to test the accuracy of empirical intermolecular potentials, because these compounds represent an example of a system where a small change in molecular geometry already induces a qualitatively different crystal packing. Lattice energy minimisations for these three compounds applying both, rigid body and flexible body approaches, are reported. The calculations quite reasonably reproduce the crystallisation behaviour observed in this heteropolymorphic series. We conclude that the state-of-the-art approach and all four tested empirical intermolecular potentials are adequate for these organometallic compounds. However, it is crucial to input the most accurate molecular structures. Molecular structures determined by X-ray analysis need to be corrected for the apparent bond shrinkage due to librational motion. When these molecular structures are to be obtained by Molecular Mechanics or Quantum Mechanics methods the highest possible accuracy is required. Our results suggest that routine polymorph prediction may be more severely hampered by inaccuracies in molecular structures than by inadequacies in the intermolecular potentials. The key to a successful structure prediction is therefore the input of reliable molecular structures.

Introduction

The last few years have seen an increasing interest in the prediction of crystal structures for various reasons. The two main motives are, on the one hand, structure solution in real space (solving the phase problem), where interpretation of the powder diffraction intensities in reciprocal space has proved impossible;[2−5] on the other hand, exploration of the lattice energy hypersurface is driven by the need for so-far-unknown polymorphs with desired properties (shelf life, solubility, bioavailability, morphology, etc.),[6−13] or even perhaps for patenting and registration purposes.

The vast majority of search engines employ lattice energies based on some empirical intermolecular atom−atom pair potentials as the cost function,[14,15] and the systems most frequently investigated are neutral organic molecules. The basic experience is that, often, many theoretical polymorphs are identified within a lattice energy range of 10 kJ/mol[16] and that the experimentally observed structure — where known — is indeed close to the global minimum. This suggests that phase space is thoroughly covered by the different search engines, but even the most elaborate and presumably accurate potentials often fail to give the experimental crystal structure always with the lowest lattice energy as would be expected for thermodynamic product control. Observation of polymorphism at the same *p,T* conditions or even in the same crystal crop indicates that, for some substances, there may indeed be a range of energetically accessible structures, and that the kinetics and thermodynamics of nucleation — about which little is known — are responsible for selecting those which will be found experimentally. However, contrary to the experience in theoretical predictions, in the experimental world polymorphism seems to be much less pervasive.[17] No one has, for instance, ever seen acetylsalicylic acid polymorphs[18] despite the large quantities of aspirin tablets manufactured.

Polymorphs may be considered as conformers of the supramolecule which is the crystal structure itself.[19] Crystal polymorphism for any one compound is therefore already a valuable and informative phenomenon with regard to supramolecular chemistry and crystal engineering. Polymorphs are the result of the same cohesive forces and therefore they should provide better information on intermolecular forces. Moreover, since it is not expected that nucleation-induced metastability is very pronounced when growing

[‡] Part 6: Ref.[1]

[a] Institut für Anorganische Chemie der Universität Regensburg, D-93040 Regensburg, Germany
Fax: (internat.) + 49-941/943-3261
E-mail: josef.breu@chemie.uni-regensburg.de
[b] Department of Medical Chemistry, Royal Danish School of Pharmacy,
Universitetsparken 2, DK-2100 Copenhagen, Denmark
Fax: (internat.) + 45-35/372-209
E-mail: peo@dfh.dk

Supporting information for this article is available on the WWW under http://www.wiley-vch.de/home/eurjic or from the author.

  1434−1948/00/1111−2409 $ 17.50+.50/0

crystals at room temperature, polymorphism may also help to assess the quality of different empirical intermolecular potentials used in structure prediction. In that respect, it is very useful if polymorphism can be tailored and/or the crystallisation of unstable polymorphs can be enforced on the system, for example, by taking advantage of chirality or tailor-made additives. In such a way, a wider lattice-energy range should be accessible experimentally. Furthermore, it is helpful if the molecule has few internal degrees of freedom that would require a balanced and accurate treatment of intra- and intermolecular parts of a force field.

The preceding paper[1] describes such a system. With $[M(bpy)_3](PF_6)_2$ (M = Ni, Zn, Ru) three different polymorphs are observed. α-$[M(bpy)_3](PF_6)_2$ is just a slight distortion of β-$[M(bpy)_3](PF_6)_2$ and the phase transition is induced upon cooling, but the packing in the γ-polymorph is drastically different: while the α- and β-form are true racemates the γ-structure is an enantiomorph.

We have performed lattice-energy minimisations of the three compounds in the different structure types, both within the rigid body and the flexible body framework. The results are analysed with regard to the self-organisation of such propeller-shaped molecules. Additionally, more general conclusions regarding the mentioned problems in structure prediction are discussed on the basis of calculated lattice energies.

Results and Discussion

When studying the relative importance of different intermolecular contributions during the self-assembly of crystals, organometallic compounds display significant advantages over organic compounds since structural molecular parameters may be tuned to a much finer degree. With $[M(bpy)_3](PF_6)_2$ the size of the complex cations and the molecular electrostatic potential (MEP) may be delicately varied by substitution of the central atom. Moreover, this variation leads to different polymorphs, and it is possible to switch between the polymorphs by choosing the right metal. With M = Fe,[20] M = Ru,[21,22] or M = Os[23,24] the racemic solutions crystallize as true racemates in the β-type. This β-type undergoes a phase transition to the closely related low temperature α-polymorph.[25,26] For M = Zn this racemic structure is not accessible experimentally. Instead, the enantiomorphous γ-type is the only modification observed. For M = Ni, crystals of both structure types are obtained concomitantly in the very same crystallization batch. Finally, since $[Ru(bpy)_3]^{2+}$ is inert towards racemisation the γ-type can be "forced" upon $[Ru(bpy)_3](PF_6)_2$ by chemical resolution prior to crystallization.

According to thermodynamics, polymorphic modifications can be at equilibrium only at the phase-transition temperature where the ΔG curves cross. The likelihood of choosing exactly this temperature for crystallization is rather slim.[27] Moreover, Gavezzotti & Filippini[17] have shown in their systematic study of crystal polymorphism that entropy differences between polymorphs of differing packing topology are never large enough to have $300\Delta S$ exceed ΔH (Note that ΔH is also dependant on temperature). They conclude that relative stability among polymorphs at room temperature can be judged on the basis of packing energy (enthalpy) alone. Consequently, it is obvious that kinetics must have a certain impact when concomitant crystallization of two polymorphs is observed at the same temperature, in the same solvent, and at the same supersaturation level. For this to happen the nucleation rates of both modifications must be similar. However, concomitantly crystallizing polymorphic modifications as observed with $[Ni(bpy)_3](PF_6)_2$ must nevertheless have energetically equivalent structures.[27] Generally, it is thought that even polymorphs obtainable at varying crystallization conditions (solvent, temperature, supersaturation) have lattice energies within 4−12 kJ/mol.[18] It is expected that for concomitantly crystallizing polymorphs this range is even smaller. Therefore, already $[Ni(bpy)_3](PF_6)_2$ provides an excellent and very demanding benchmark for the validation of interatomic potentials as they must reproduce the near equivalency of the crystal energetics. The crystallization behaviour of the heteropolymorphic series of $[M(bpy)_3](PF_6)_2$ structures as a whole is even better suited to test the accuracy of empirical intermolecular atom−atom pair potentials: It is anticipated that the calculated lattice energies for β-$[Ni(bpy)_3](PF_6)_2$ and for γ-$[Ni(bpy)_3](PF_6)_2$ are very similar, irrespective of the unknown absolute value. For $[Ru(bpy)_3](PF_6)_2$ the racemic β-type, and for $[Zn(bpy)_3](PF_6)_2$ the enantiomorphic γ-type, should be preferred energetically.

Rigid-Body Minimisations

Lattice-energy minimisations for these three compounds applying the rigid body code MPA[9] (Molecular Packing Analysis) in combination with four popular sets of intermolecular potentials, CFF91,[28] Williams,[29] UNI,[30] and MM3,[31] yield very satisfying results (Tables 1−4).

In a first approximation, the quality of a set of intermolecular atom−atom pair potentials for crystal structure calculations can be judged by relaxing the experimental structures in the force field. When the experimental structure does not change much upon minimising, the intermolecular potentials are considered adequate. For a high quality set of potentials small shifts of 1−2% in the cell edges are reasonable, since this is the typical range of thermal expansion. Judging by this criterion, all experimentally observed crystal structures (EXPTL crystal model) of both structure types are satisfactorily reproduced by any of the four sets of intermolecular potentials. The maximum relative error in cell lengths is 2.2% (Table 1−4). Because our calculations neglect thermal vibrations, a shrinkage of cell lengths would have been expected. Actually, we observe quite a few cell expansions upon relaxation. This is due to the fact that, with the exception of β_{294}-$[Ru(bpy)_3](PF_6)_2$, all crystal structures were determined at low temperatures. Nevertheless, with "true 0 K" empirical intermolecular potentials, a shrinkage due to the effect of thermal expansion would still be expected, since the experimental temperatures are always

Table 1. Rigid-body lattice-energy minimisations, CFF91[28] potentials

	$[Ru(bpy)_3](PF_6)_2$				$[Ni(bpy)_3](PF_6)_2$			$[Zn(bpy)_3](PF_6)_2$	
	α_{105}[a]	β_{294}[b]	β_{200}[c]	γ_{200}[c]	β_{240}[c]	$\gamma_{200}(1)$[c]	$\gamma_{200}(2)$[c]	β[d]	γ_{200}[c]
EXPTL crystal model:									
$(a-a_{exp})/a_{exp}$ [%]	−0.6	−1.6	−1.0	−0.4	−1.3	−0.4	−0.4	–	−0.6
$(c-c_{exp})/c_{exp}$ [%]	+1.5	−1.0	+0.7	−0.2	0.0	−0.8	−0.5	–	0.0
$(V-V_{exp})/V_{exp}$ [%]	+0.3	−4.2	−1.3	−1.0	−2.6	−1.6	−1.3	–	−1.1
$E_{Inter.}$[kJ/mol][e]	−1287.3	−1291.4	−1289.4	−1278.2	−1288.5	−1285.6	−1286.0	−1261.1	−1279.9
CORR crystal model:									
$(a-a_{exp})/a_{exp}$ [%]	−0.6	−1.6	−1.0	−0.1	−1.2	+0.0	0.0	–	−0.1
$(c-c_{exp})/c_{exp}$ [%]	+1.9	0.2	+1.2	0.3	+0.6	−0.1	−0.1	–	+0.1
$(V-V_{exp})/V_{exp}$ [%]	+0.6	−3.1	−0.8	0.1	−1.8	−0.1	0.0	–	+0.0
$E_{Inter.}$[kJ/mol][e]	−1284.2	−1280.2	−1283.1	−1266.3	−1280.2	−1274.8	−1274.0	−1255.1	−1270.0

[a] Ref.[25] – [b] Ref.[21,22] – [c] Ref.[1] – [d]Hypothetical. – [e] Per mol $[M(bpy)_3](PF_6)_2$.

Table 2. Rigid-body lattice-energy minimisations, Williams[29][78] potentials

	$[Ru(bpy)_3](PF_6)_2$				$[Ni(bpy)_3](PF_6)_2$			$[Zn(bpy)_3](PF_6)_2$	
	α_{105}[a]	β_{294}[b]	β_{200}[c]	γ_{200}[c]	β_{240}[c]	$\gamma_{200}(1)$[c]	$\gamma_{200}(2)$[c]	β[d]	γ_{200}[c]
EXPTL crystal model:									
$(a-a_{exp})/a_{exp}$ [%]	0.3	−0.8	−0.1	−0.1	−0.5	0.0	0.0	–	0.0
$(c-c_{exp})/c_{exp}$ [%]	1.5	−1.1	0.4	0.1	−0.2	−0.1	−0.2	–	0.0
$(V-V_{exp})/V_{exp}$ [%]	2.1	−2.6	0.2	0.0	−1.2	0.0	−0.1	–	0.0
$E_{Inter.}$[kJ/mol][e]	−1165.6	−1170.2	−1168.3	−1166.1	−1167.9	−1173.0	−1173.5	−1146.8	−1168.5
CORR crystal model:									
$(a-a_{exp})/a_{exp}$ [%]	0.3	−0.6	0.0	0.4	−0.3	0.4	0.4	–	0.3
$(c-c_{exp})/c_{exp}$ [%]	1.7	−0.2	1.0	0.4	0.4	0.0	0.2	–	0.3
$(V-V_{exp})/V_{exp}$ [%]	2.4	−1.5	1.0	1.2	−0.2	0.7	1.0	–	0.9
$E_{Inter.}$[kJ/mol][e]	−1162.8	−1160.2	−1162.7	−1156.4	−1160.6	−1163.7	−1163.1	−1141.4	−1160.0

[a] Ref.[25] – [b] Ref.[21,22] – [c] Ref.[1] – [d] Hypothetical. – [e] Per mol $[M(bpy)_3](PF_6)_2$.

Table 3. Rigid-body lattice-energy minimisations, UNI[30] potentials

	$[Ru(bpy)_3](PF_6)_2$				$[Ni(bpy)_3](PF_6)_2$			$[Zn(bpy)_3](PF_6)_2$	
	α_{105} [a]	β_{294}[b]	β_{200}[c]	γ_{200}[c]	β_{240}[c]	$\gamma_{200}(1)$[c]	$\gamma_{200}(2)$[c]	β[d]	γ_{200}[c]
EXPTL crystal model:									
$(a-a_{exp})/a_{exp}$ [%]	0.7	−0.3	0.4	0.8	0.1	0.9	1.0	–	0.7
$(c-c_{exp})/c_{exp}$ [%]	2.2	−0.4	0.9	0.6	0.2	0.3	0.2	–	0.8
$(V-V_{exp})/V_{exp}$ [%]	3.7	−1.0	1.7	2.2	0.4	2.2	2.1	–	2.3
$E_{Inter.}$[kJ/mol][e]	−1151.1	−1155.0	−1153.5	−1148.2	−1153.1	−1155.3	−1155.7	−1132.7	−1151.2
CORR crystal model:									
$(a-a_{exp})/a_{exp}$ [%]	0.8	−0.1	0.6	1.2	0.2	1.3	1.3	–	1.2
$(c-c_{exp})/c_{exp}$ [%]	2.3	0.2	1.3	0.9	0.9	0.7	0.7	–	0.8
$(V-V_{exp})/V_{exp}$ [%]	4.0	0.0	2.5	3.4	1.3	3.2	3.3	–	3.1
$E_{Inter.}$[kJ/mol][e]	−1148.5	−1145.5	−1148.1	−1138.9	−1146.2	−1146.5	−1145.9	−1127.5	−1143.2
$\Delta E_{Coul.}$ [kJ/mol]			11.6		13.9			16.5	
$\Delta E_{d/r}$ [kJ/mol]			−20.8		−14.0			−0.8	

[a] Ref.[25] – [b] Ref.[21,22] – [c] Ref.[1] – [d] Hypothetical. – [e] Per mol $[M(bpy)_3](PF_6)_2$.

Table 4. Rigid-body lattice-energy minimisations, MM3[31] potentials

	$[Ru(bpy)_3](PF_6)_2$				$[Ni(bpy)_3](PF_6)_2$			$[Zn(bpy)_3](PF_6)_2$	
	α_{105}[a]	β_{294}[b]	β_{200}[c]	γ_{200}[c]	β_{240}[c]	$\gamma_{200}(1)$[c]	$\gamma_{200}(2)$[c]	β[d]	γ_{200}[c]
EXPTL crystal model:									
$(a-a_{exp})/a_{exp}$ [%]	0.6	−0.3	0.4	0.6	0.0	0.7	0.8	0.4	0.7
$(c-c_{exp})/c_{exp}$ [%]	1.7	−1.2	0.3	−0.1	−0.2	−0.2	−0.1	3.5	0.1
$(V-V_{exp})/V_{exp}$ [%]	2.9	−1.8	1.1	1.2	−0.1	1.3	1.4	4.3	1.5
$E_{Inter.}$[kJ/mol][e]	−1101.8	−1105.2	−1104.3	−1101.4	−1099.4	−1102.2	−1102.7	−1082.1	−1097.1
CORR crystal model:									
$(a-a_{exp})/a_{exp}$ [%]	0.6	−0.1	0.4	1.0	0.1	1.1	1.1	0.5	0.8
$(c-c_{exp})/c_{exp}$ [%]	2.0	−0.4	0.8	0.4	0.5	0.0	0.3	3.7	0.6
$(V-V_{exp})/V_{exp}$ [%]	3.2	−0.6	−1.6	2.4	0.6	2.1	2.5	4.8	2.3
$E_{Inter.}$[kJ/mol][e]	−1099.7	−1097.4	−1099.9	−1094.2	−1093.8	−1095.4	−1095.1	−1077.9	−1090.7

[a] Ref.[25] – [b] Ref.[21,22] – [c] Ref.[1] – [d] Hypothetical. – [e] Per mol $[M(bpy)_3](PF_6)_2$.

well above 0 K. However, although temperature is not explicitly considered, some thermal effects have been subsumed into the interatomic potentials during their fitting to experimental observables which were mostly determined at room temperature. As discussed in more detail by Gale,[32] modern-day potentials correspond to an effective temperature which is a weighted average of the temperatures at which the different pieces of data were measured. The simulations therefore should rather be called athermal, and this might explain the observed cell expansions upon relaxation.

The lattice energies calculated for the three compounds $[M(bpy)_3](PF_6)_2$ (M = Ru, Ni, Zn) in the two basic structure types (β and γ) cover only a small energy range despite the drastically differing packing topology. This result, in combination with the uncertainty in the model potential would render it impossible to estimate the relative stability of the two polymorphs of any singular compound and the reliability of such a conclusion without further evidence. However, we can take advantage of the additional observation that only the Ni compound crystallizes concomitantly in both structure types. Therefore, for $[Ni(bpy)_3](PF_6)_2$ both structure types are expected to be energetically equivalent, while for $[Zn(bpy)_3](PF_6)_2$ the γ-type, and for $[Ru(bpy)_3](PF_6)_2$ the β-type, should be energetically favoured. It is a very fortunate coincidence that, within this series of complexes, it is possible to switch between the two topologically different polymorphs by simply substituting the central metal atom. If this experimentally observed crystallization behaviour within this unique heteropolymorphic series of $[M(bpy)_3](PF_6)_2$ (M = Ru, Ni, Zn) compounds is reflected in the predicted relative stability of the two polymorphs, even small lattice-energy differences may be regarded as significant. Furthermore, since the transition between the α- and the β-structure for $[Ru(bpy)_3](PF_6)_2$ is driven by cooling and therefore by entropy, a "0 K" static lattice energy minimisation should predict the α-structure to be more stable.

Judging by this energy criterion all four sets of empirical intermolecular potentials perform well again. The maximum energy difference between the γ- and the β-structure for the Ni compound is observed with the Williams potentials (5.1 kJ/mol, Table 1−4, EXPTL crystal model). Also, all four potential sets predict the relative stability of the two polymorphs for the Ru and the Zn compound correctly. However, for the Williams, the UNI, and the MM3 potential sets, the β- and γ-structures for $[Ru(bpy)_3](PF_6)_2$ are getting almost as close in energy as for $[Ni(bpy)_3](PF_6)_2$. None of the intermolecular potential sets predicts α-$[Ru(bpy)_3](PF_6)_2$ to be lower in energy than β-$[Ru(bpy)_3](PF_6)_2$.

Although all four intermolecular force fields have been calibrated by using some experimentally determined sublimation enthalpies, the absolute values for the calculated lattice energies differ considerably (up to 15%).

It is difficult to quantify precisely the uncertainties associated with this rigid body approach. The lattice energies as defined by the intermolecular interactions are rather sensitive to the particular rigid molecular structures (see also next two sections) that are put into the starting configuration. These molecular structures may vary due to experimental errors and, more importantly, due to tiny conformational changes induced by the interplay of intramolecular and intermolecular forces, which in turn is dependant on temperature. To explore the effect of such methodical uncertainties in the molecular structures on the results of the lattice energy minimisations, the lattice energy for γ-$[Ni(bpy)_3](PF_6)_2$ was calculated for two starting structures which were determined at the same temperature (200 K) using two data sets sampled on different crystals [$\gamma_{200}(1)$ and $\gamma_{200}(2)$[1]]. The lattice energies for these two starting structures determined at the same temperature differ by less than 0.5 kJ/mol. To investigate minor modifications in the molecular shapes induced by temperature-dependant packing requirements the lattice energy for the racemic $[Ru(bpy)_3](PF_6)_2$ structures was not only calculated for the α-type (105 K, α_{105})[25] and the β-structure determined by Rillema at 294 K (β_{294}),[22] but also for a structure determined at an intermediate temperature (200 K, β_{200}),[1] that is still well above the onset of the phase transition to the low-temperature modification. The variation of the calculated lattice energies increases by up to 2 kJ/mol. Since the lattice energies are compared for structures determined at different temperatures, this may be regarded as the error in the intermolecular lattice energy inherent in this rigid body approximation.

Influence of Systematic Errors in Molecular Structures

Next, the effect of a systematic error on lattice energies calculated within the rigid body approach shall be taken into account which is contained in input molecular structures determined by X-ray structure analysis. Cruishank noted as early as 1956 that rotational oscillations of rigid molecules or moieties in crystals cause the apparent atomic positions to be slightly displaced from the true position towards the rotation axis.[33] X-ray analysis locates the centroids of atomic distributions that are undergoing vibrations. Distances calculated from these mean positions are shorter and cannot be interpreted directly as interatomic distances.

Approximately spherical molecules like $[PF_6]^-$ are especially prone to be affected by this systematic error. When comparing Ru−N distances as determined by different structure determinations of $[Ru(bpy)_3](PF_6)_2$ with the corresponding P−F bond lengths (Table 5) it is striking that the variation in bond length is up to an order of magnitude larger in the complex anion than in the cation.

From the principal axis directions and mean-square libration amplitudes (eigenvectors and eigenvalues of $\boldsymbol{L}$) calculated from the anisotropic displacement parameters reported for $LiPF_6$ [34] a true experimental bond length of 1.61 Å can be estimated for the P−F bond in $[PF_6]^-$. From a comparison with the uncorrected values a considerable shrinkage effect due to librational motion is evident. The apparent shortening of the P−F bond as observed in structure determinations of $[Ru(bpy)_3](PF_6)_2$ can be up to 0.08 Å. Thus the molecular dimension of the hexafluorophosphate anion obtained by X-ray crystal structure analysis is considerably in error unless corrected for the effect of mo-

Table 5. Variance of Ru−N and P−F distances in different structure determinations of $[Ru(bpy)_3](PF_6)_2$

Structure type	β_{294}[a]	β_{200}[b]	α_{105}[c]			γ_{200} [b]
Site symmetry	D_3	D_3	C_3			C_1
Independ. site			A	B	C	
Ru−N [Å]	2.056	2.048	2.052 2.053	2.053 2.053	2.053 2.053	2.049 – 2.069
P−F [Å]	1.549 1.568	1.570 1.593		1.583 – 1.618		1.527 – 1.614

[a] Ref.[21,22] – [b] Ref.[1]. – [c] Ref.[25]

lecular libration. Since the complex cations are effected to a much lesser extent by molecular libration, no corrections were applied to their molecular shape. When expanding the P−F vector in the starting structures to a reasonable value of 1.61 Å (CORR crystal model) considerable shifts in the calculated lattice energies are observed (Table 1−4). The maximum shift as compared to the EXPTL crystal model is observed for γ-$[Ru(bpy)_3](PF_6)_2$ in connection with the CFF91 potentials and amounts to 11.9 kJ/mol. When recalling that 10 kJ/mol is an energy range within which, usually, many theoretical polymorphs are predicted, it becomes obvious that correction of the observed molecular structure does indeed matter and should not be neglected.

Also, calculated lattice energies are in much better agreement with the observed crystallization behaviour for the CORR crystal model than for the EXPTL crystal model. The energy differences between β-$[Ni(bpy)_3](PF_6)_2$ and $\gamma_{200}(1)$-$[Ni(bpy)_3](PF_6)_2$ become 5.4 kJ/mol, 3.1 kJ/mol, 0.3 kJ/mol and 1.6 kJ/mol for the CFF91, Williams, UNI, and MM3 potentials, respectively. All four sets of empirical intermolecular potentials predict the γ-type to be significantly lower in energy than the β-type for $[Zn(bpy)_3](PF_6)_2$. β-$[Ru(bpy)_3](PF_6)_2$ is not only predicted to be more stable than γ-$[Ru(bpy)_3](PF_6)_2$, the energy gap between the two structure types also increases after applying the correction. Moreover, the CFF91, Williams, and UNI potentials even predict α-$[Ru(bpy)_3](PF_6)_2$ to be slightly more stable (100−400 J) than β_{200}-$[Ru(bpy)_3](PF_6)_2$.

Although the dispersion/repulsion parameters used with the four tested intermolecular force fields have not been optimised for this class of organometallic compounds, the potentials yield an excellent agreement with experiment. The atom centred monopoles give an accurate enough description of the electrostatic potential, and even anisotropic electrostatic interactions, such as the important π−π interactions, are satisfactorily represented. Quadrupole−quadrupole interactions from the π electrons are not explicitly included into the electrostatic model, but they get subsumed into the monopole−monopole interactions. Also, the assumed isotropic atom−atom form for the repulsion appears to be adequate to describe the stacking of aromatic rings as observed in the γ-structure[1] even though the charge density in these regions is known not to be spherical.[35]

This satisfying result encourages further interpretation with respect to crystal engineering. Recognition of special interactions and recurring intermolecular motifs in molecular crystals offers the opportunity of classification, but quantifying the interaction strengths provides a deeper understanding than sheer geometry — there is no such thing as a pure and simple structure-defining interaction. With respect to the intermolecular interaction patterns the β- and γ-structure differ most significantly in the particular C−H···π-interaction realised. In the β-modification T-shaped π−π interaction[36−38] contacts along the racemic columns with colinear C_3 axes are observed, while in the γ-type shifted π-stacks occur along the complex cation columns running along *c* (Figure 5a and 5c in ref.[1] respectively). Since these two mutual arrangements also allow for an effective penetration of adjacent molecules, it cannot even be decided from geometry alone whether these C−H···π-interactions have to be realised or just happen to be there because of the complementarity of molecular surfaces and thus packing efficiency. It is unclear whether the dispersion/repulsion- or the electrostatic C−H···π-interactions are predominantly responsibly for these two intermolecular interaction patterns. As the implied energies are small, a sound proof of this cannot be given without quantitative calculations. The calculated lattice energies may therefore be used to examine the relative strength, energetics and structural influence of these two different intermolecular interactions.

A comparison of the relative size of the dispersion/repulsion ($\Delta E_{d/r}$) and the electrostatic ($\Delta E_{Coul.}$) contribution to the total lattice energy is revealing with respect to the relative significance of the C−H···π-interactions (Table 3, CORR crystal model). On one hand, the Coulomb energy would prefer the γ-structure for all three compounds. This is not provoked by the arrangement of the ions, which in fact is very similar in both structures and would actually give a larger Coulomb energy for the β-arrangement: putting charges of +2 and −1 at the corresponding positions of the Ru and the P atom gives Madelung energies of −1000.4 kJ/mol and −998.0 kJ/mol for the β_{200}- and γ-arrangement, respectively. Consequently, the electrostatic preference of the γ-type must be founded in local electrostatic contributions, i.e. C−H···π- or C−H···F-interactions. Unfortunately, these two cannot be further separated. The differing MEPs for the three cations contribute towards the observed differences in $\Delta E_{Coul.}$. On the other hand, the dispersion/repulsion contribution to the total lattice energy favours the β-type for all three compounds. The differing size of the complex cations is subsumed into this energy term via the repulsion. While $\Delta E_{Coul.}$ increases moderately when going from $[Ru(bpy)_3](PF_6)_2$ to $[Ni(bpy)_3](PF_6)_2$ and to $[Zn(bpy)_3](PF_6)_2$, $\Delta E_{d/r}$ drops sharply. With large cations (e.g. M = Zn) only the γ-type, and with small cations (e.g. M = Fe, Ru) only the β-type, is observed. By chance the differences happen to cancel with M = Ni and consequently both structures crystallize concomitantly. Although the

C−H···π- and C−H···F-contributions to the Coulomb energy cannot be separated, these results indicate that C−H···π-interactions have a larger relative weight in the concert of intermolecular interactions in the shifted π-stack geometry realised in the γ-structure than in the T−shaped (edge-to-face) arrangement in the β-structure. This result contradicts the importance assigned by Dance[39] to such concerted T-shaped arrangements with regard to the molecular recognition between $[M(bpy)_3]^{n+}$. This supramolecular motif was even given a distinct name, "sextuple aryl embrace". Instead, our lattice energy calculations are in line with the experimental evidence presented by Wilcox[40,41] that suggests that the electrostatic potential of the aromatic ring is *not* a dominant aspect of the edge-to-face aryl−aryl interaction, but that London dispersion forces should be the predominant driving force for this type of interaction.

However, it should be kept in mind that the experimental crystal structures cannot be explained by a single type of interaction but result from an interplay between all the different interactions, both weak and strong.

Flexible Body Minimisations

From a comparison of the lattice energies calculated for β_{200}-$[Ru(bpy)_3](PF_6)_2$ and β_{294}-$[Ru(bpy)_3](PF_6)_2$ it is already evident that even the very limited conformational flexibility inherent in $[M(bpy)_3]^{2+}$ does play some role and that the subtle interplay between the molecular structure and the crystal structure may be significant even for these rather rigid molecules. When molecules are conformationally flexible, the intramolecular energy difference between the two solid phases has to be included in the total energy, since the crystal structure molecular conformers are not necessarily the lowest energy conformers.[42,43] However, this requires an accurate balance between inter- and intramolecular potentials.

To get an idea of the significance of the intramolecular term, we have performed single-point density-functional calculations, although there are justified concerns about calculating the relative stability of conformers using ab initio methods on molecules with a fixed geometry.[42] Such single-point calculations are very sensitive to slight errors in the experimental bond lengths and angles. These errors may be of varying magnitude for different structure determinations and, consequently, this will bias the results in an unpredictable way. However, α-$[Ru(bpy)_3](PF_6)_2$ offers the rare opportunity of three crystallographically independent complex cation sites with slightly varying molecular shapes (see intramolecular parameters given in Table 6), which should be of comparable accuracy. These three sites differ most significantly in the torsional angles around the pyridine−pyridine bond (py−py). The ab initio energies for the three different crystallographic sites in the gas phase already differ by 5.3 kJ/mol which is of similar magnitude to the lattice-energy differences observed in the rigid body approach. This result suggests that one might have to worry about intramolecular contributions even though $[M(bpy)_3]^{2+}$ cations display only very limited conformational flexibility.

Unfortunately, reliable molecular mechanics parameters for Ru^{II}−polypyridyl coordination compounds have up to now only been developed within the context of the MM3* force field in MacroModel.[44] However, this package does not allow lattice-energy calculations with accelerated convergence techniques. Therefore, we derived molecular mechanics parameters within the context of the CFF91 force

Table 6. Molecular geometries and (cluster) energies of the independent cation sites in α-$[Ru(bpy)_3](PF_6)_2$ [25]

Independent site	A	B	C
M−N [Å]	2.052	2.053	2.053
	2.053	2.053	2.053
μ [°][a]	78.65	78.56	78.59
[°][a]	89.51	89.88	89.90
ν [°][a]	95.05	96.56	96.77
	97.18	95.44	95.17
np_{xyz}−cpp−cpp−np_{xyz} [°][a]	6.02	4.61	8.39
cp−cpp−cpp−cp [°][a]	11.53	13.07	6.74
py−py [°][a]	9.73	10.26	9.01
ligand bite [Å][a]	2.601	2.599	2.601
b[b]	1.267	1.266	1.267
2Θ [°][c]	51.2	51.1	51.5
μ−t1 [Å][d]	1.074	1.067	1.026
μ−t2 [Å][d]	1.036	1.041	1.075
t1−M−t2 [°]	180.0	180.0	180.0
S [Å][e]	3.051[f]	3.051[f]	3.053[f]
$A = \alpha_1 + \alpha_2$ [°][a]	228.7	228.7	228.6
$B = \beta_1 + \beta_2$ [°][a]	247.6	246.9	247.7
Δ_{max} [Å][g]	0.037	0.037	0.018
E(DMol) [kJ/mol]	−29618.8	−29618.8	−29624.1
$E_{rel.}$(DMol) [kJ/mol]	5.3	5.3	0
E(CFF91) [kJ/mol]	118.8	118.4	117.6
$E_{rel.}$(CFF91) [kJ/mol]	1.2	0.8	0

[a] For labelling scheme see Figure 1. − [b] Normalised ligand bite. − [c] Trigonal twist. − [d] Distances between the central atom and the centre of gravity of the trigonal faces formed by N atoms of the bpy ligands. − [e] Edge length of the basis of the trigonal antiprism. − [f] Averaged in D_3−symmetry. − [g] Maximum deviation from the best plane within a single pyridine ring.

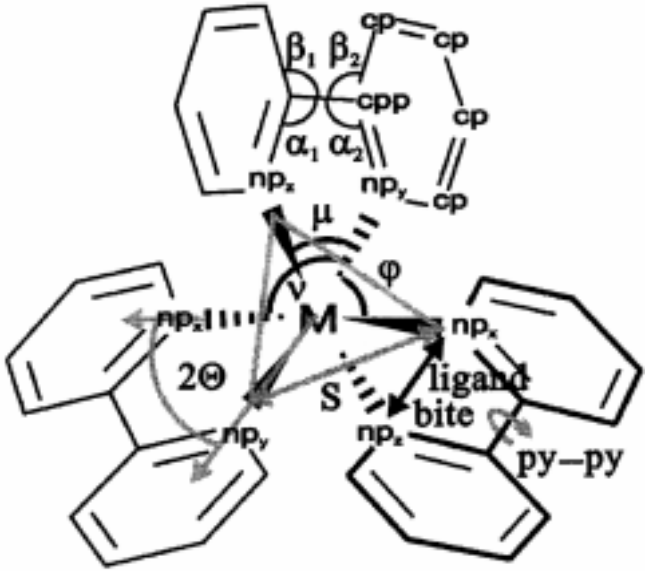

Figure 1. Labelling scheme of geometrical parameters and atom types listed in the Tables

field, which subsequently permits lattice energy minimisations employing Cerius−OFF.[45] This program uses Ewald summation methods for evaluation of the electrostatic- and the dispersion term yielding lattice energies of the same precision as obtained by MPA in the rigid body approach.

In order to accurately reproduce structures and energies by a molecular mechanics force field, information about the exact shape of the intramolecular potential energy surface (PSE) has to be used in the fitting of the force field.[46] Mass weighted Hessian elements calculated by Quantum Mechanics (QM) supply a wealth of information about the PSE and can be included very efficiently in parametrizations. However, it is important to realise that systematic errors in the QM method will be reproduced by the force field. This may be counteracted by simultaneous use[44,46−49] of structural information contained in experimentally determined molecular structures. Here, it should be kept in mind that these structures might be influenced by crystal packing[50] and by systematic errors caused by thermal motion, as discussed earlier. The relative weighting factors for QM and experimental "observables" employed in the fitting of the Ru force field parameters (Table S8) and the optimised parameters (Tables S9−S12) are given in the supporting information.

Unfortunately, there are not enough reliable experimental parameters available in the literature that could be used in the parametrization of the anion (see discussion in the previous section). Furthermore, density functional methods applied to $[PF_6]^-$ in the gas phase give equilibrium bond lengths that are longer (1.648 Å) than the values observed in crystal structures. Therefore, the equilibrium bond length has to be shifted after fitting (r_0 = 1.61 Å). The optimised force-field parameters for $[PF_6]^-$ are also listed in the supporting information (Table S13).

The ab initio energies calculated for the three independent sites in α-$[Ru(bpy)_3](PF_6)_2$ may be used as a first benchmark that might confirm the accuracy of the derived force field. DMol[53] and CFF91 energies are indeed consistent (Table 6), suggesting that, to a first approximation, the intramolecular potential energy landscape is adequately described by the force field. Structural overlays of molecular structures as observed in the two crystal structures and as minimised in the context of the force field show only minor deviations (Figure 2) and indicate that intra- and intermolecular interactions are quite satisfactorily balanced.

Nevertheless, the flexible-body model fails to produce the correct order in lattice energies for β_{200}-$[Ru(bpy)_3](PF_6)_2$ and γ-$[Ru(bpy)_3](PF_6)_2$. The energy difference between the γ- and the β-type drops from 16.8 kJ/mol to −8.5 kJ/mol when going from the rigid body to the flexible body model (Table 1, CORR crystal model and Table 7). At first glance the optimised unit-cell dimensions are still in satisfying agreement with those determined by experiment. Also, the experimental intramolecular parameters listed in Table 8 are well reproduced. There is only one py−py torsion in the γ-modification that stands out by differing by 8.1° from the experimental value. The valence terms of the energies are

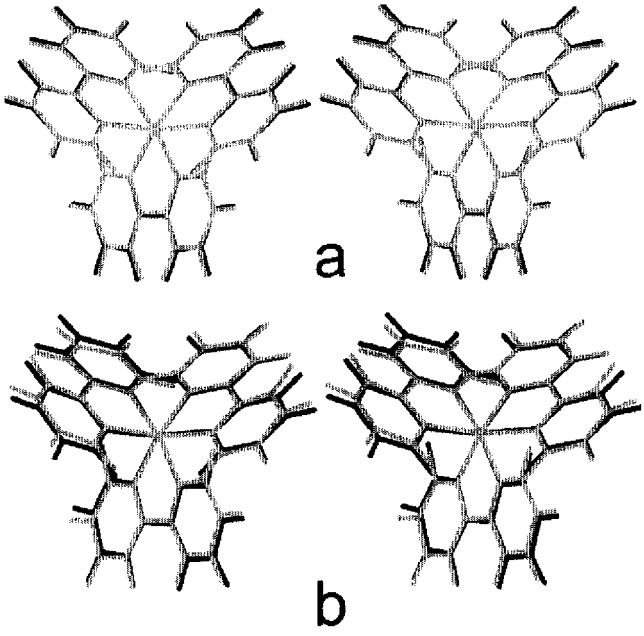

Figure 2. Stereo view of overlayed experimental (black) and molecular mechanics minimised (grey) molecular structures of $[M(bpy)_3]^{2+}$ in the β- (a) and γ-modification (b), respectively

Table 7. Flexible-body lattice-energy minimisations, CFF91 potentials

	β_{200}	γ_{200}
$(a - a_{exp})/a_{exp}$ [%]	−0.5	+0.4
$(c - c_{exp})/c_{exp}$ [%]	2.6	−2.2
$(V - V_{exp})/V_{exp}$ [%]	+1.7	−1.4
E_{Total} [kJ/mol][a]	−857.7	−866.2
$E_{Coul.}$[kJ/mol][a]	−544.2	−558.2
$E_{Disp./Rep.}$[kJ/mol][a]	−349.6	−344.3
$E_{Valence}$[kJ/mol][a]	36.1	36.3
$E_{Inter.}$[kJ/mol][a] [b]	−1280.4	−1290.8

[a] Per mol $[M(bpy)_3](PF_6)_2$. − [b] Calculated employing MPA.

actually very similar in both polymorphs (36.1 kJ/mol and 36.3 kJ/mol for β- and γ-type, respectively).

The decisive change when going from the rigid- to the flexible-body model happens in the intermolecular energy [note that the nonbonding energies calculated in the molecular mechanics approach (Table 7) contain intramolecular contributions!]. While the intermolecular lattice energy as calculated with MPA for the flexible body minimised β_{200}-$[Ru(bpy)_3](PF_6)_2$ structure is very similar to the one observed in the rigid body approach (−1280.4 kJ/mol versus −1283.1 kJ/mol), it changes considerably for flexible body minimised γ-$[Ru(bpy)_3](PF_6)_2$ (−1290.8 kJ/mol versus −1266.3 kJ/mol). When taking a closer look at both the intra- and the intermolecular parameter differences (Table 8 and 9), an interesting correlation becomes evident. In comparison to the experimentally observed molecular structure in the γ-type, the relaxed cation is somewhat higher along the pseudo−C_3 axis as indicated by the M−t1 and M−t2 distances (1.102 Å and 1.103 Å) and slightly thinner perpendicular to it (S = 3.012 Å). In other words, the cation is stretched out along the pseudo-C_3 axis. Since the pseudo-

Table 8. Comparison of experimental (exp.) and flexible-body-minimised (fmin., CFF91 force field, Cerius−OFF) intramolecular geometrical parameters for $[Ru(bpy)_3](PF_6)_2$

	β_{200}^{exp}	β_{200}^{fmin}	$\gamma\cong_{200}^{exp}$	$\gamma\cong_{200}^{fmin}$
M−N [Å]	2.048(2)	2.045	2.058(4)	2.057
			2.065(3)	2.061
			2.066(4)	2.060
			2.067(4)	2.060
			2.061(3)	2.061
			2.063(4)	2.057
μ [°][a]	78.74(8)	80.29	79.29(12)	80.16
			78.41(15)	79.85
			79.14(12)	80.17
[°][a]	89.51(9)	90.44	92.12(16)	93.37
			91.40(12)	92.17
			89.36(13)	92.17
ν [°][a]	96.08(9)	94.82	94.78(15)	93.51
			95.43(13)	92.56
			96.75(13)	95.93
			93.43(12)	92.55
			94.95(16)	93.51
			96.59(12)	95.93
ligand bite[A][a]	2.598(3)	2.637	2.631(5)	2.651
			2.612(5)	2.644
			2.627(5)	2.651
b[b]	1.269(2)	1.289	1.271(4)[c]	1.286[c]
2Θ [°][d]	51.6(1)	51.9	50.5(2)[c]	49.9[c]
μ−t1 [Å][e]	1.050(4)	1.077	1.068(4)	1.102
μ−t2 [Å][e]	1.050(2)	1.077	1.082(4)	1.103
t1−M−t2 [°]	180.0	180.0	179.3(2)	179.3
S [Å][f]	3.046(3)	3.011	3.050[c]	3.012[c]
py−py [°][a]	8.81(13)	10.58	6.7(2)	14.8
			9.4(2)	8.1
			12.7(3)	14.8
$\alpha_1 + \alpha_2$ [°][a]	228.9(4)	233.0	230.0(7)	233.7
			229.4(8)	233.5
			230.7(7)	233.7
$\beta_1 + \beta_2$[°][a]	247.9(4)	244.2	246.4(8)	242.4
			247.7(8)	243.4
			246.3(8)	242.5
Δ_{max} [Å][g]	0.019(2)	0.032	0.028(4)	0.028

[a] For labelling scheme see Figure 1. − [b] Normalised ligand bite. − [c] Averaged in D_3−symmetry. − [d] Trigonal twist. − [e] Distances between the central atom and the centre of gravity of the trigonal faces formed by N atoms of the bpy ligands. − [f] Edge length of the basis of the trigonal antiprism. − [g] Maximum deviation from the best plane within a single pyridine ring.

C_3 axes of the complex cations in the γ-type lie approximately in the *ab* plane, the *a* and *b* axes expand upon minimisation in the context of the flexible body force field, while the *c* axis shrinks relative to the experimental values. In the rigid-body minimisation it is the other way around. As a consequence the cation−cation distance along the columns is too short by 0.2 Å (Table 9). The prominent change in one of the py−py torsions is probably the outgrowth of an intramolecular adjustment to this alteration in intermolecular geometry. Even though other small distortions occur to the molecular shape upon minimisation, it appears that changing this critical molecular parameter of relative height by a tiny amount of a few hundredths of an angström already induces a different ranking of the two polymorphs. As a consequence, one has to realize that a successful crystal structure prediction requires an accuracy in the determination of the underlying molecular shape that certainly overtaxes the best force fields and even QM methods currently available. Apparently, some force constants for intramolecular distortions are predicted to be too weak in the DFT calculations. Consequently, errors are introduced in the MM force field, since the force field cannot give better results than the data that went into its derivation. It should be noted that, due to its corrugated shape, $[Ru(bpy)_3]^{2+}$ displays quite a few intramolecular inter-ligand contacts which are less than the van der Waals separation. Therefore, the electron-density distribution in these rather remote inter-ligand regions needs to be represented accurately in order to get a realistic picture of nonbonding intramolecular contributions to the PES, which in turn greatly influence the relative positions of the ligands. It is a well-known fact that present day DFT is struggling with the long-range behaviour of the electron density.[54,55]

Table 9. Comparison of experimental (exp.), rigid-body- (rmin., CFF91 force-field, MPA), and flexible-body-minimised (fmin., CFF91 force-field, Cerius-OFF) intermolecular geometrical parameters for $[Ru(bpy)_3](PF_6)_2$

	β_{200}^{exp}	β_{200}^{rmin}	β_{200}^{fmin}	$\gamma\cong_{200}^{exp}$	$\gamma\cong_{200}^{rmin}$	$\gamma\cong_{200}^{fmin}$
M···M_{column} [Å]	8.1494(5)	8.247	8.363	8.7601(6)	8.782	8.559
M···M_{layer} [Å]	10.6453(6)	10.542	10.596	10.3809(7)	10.373	10.427
M···P [Å]	6.4422(5)	6.365	6.431	6.281(2)	6.279	6.445
				6.249(2)	6.248	6.445
				6.389(1)	6.387	6.621
				6.500(2)	6.498	6.332
				6.802(2)	6.800	6.332
				6.845(2)	6.843	6.621

Conclusions

Polymorphism may be of considerable benefit to crystal engineering. Polymorphic systems provide unique opportunities to study the competition between different intermolecular interaction patterns and correlations between changes in molecular structure and crystal packing. This is especially true if concomitant crystallization is observed.

Our calculations reproduce quite reasonably the crystallization behaviour observed in this heteropolymorphic system of $[M(bpy)_3](PF_6)_2$ (M = Ru, Ni, Zn). We conclude that the state-of-the-art approach and all four tested sets of empirical intermolecular atom−atom pair potentials are adequate for this class of organometallic compounds. When starting with the most accurate crystal structures, determined at low temperature and corrected for apparent bond shrinkage due to librational motion, significantly lower lattice energies are calculated for the experimentally observed packing topologies. Where two polymorphs crystallize concomitantly, similar lattice energies result for both structures. However, since the rigid body approach requires molecular geometries from crystal structure determinations it involves no predictive power.

A comparison of the relative size of the dispersion/repulsion ($\Delta E_{d/r}$) and the electrostatic ($\Delta E_{Coul.}$) contribution to the total lattice energy suggests that the electrostatic potential of the aromatic ring is *not* a dominant aspect of the edge-to-face aryl−aryl interaction. Certainly, concerted T-

shaped arrangements are not the electrostatically favoured molecular recognition motif between $[M(bpy)_3]^{n+}$.

The essence of the crystal structure prediction difficulties is the close proximity of several possible crystal structures for the same compound. The investigated compounds represent a good example of a system where a small change in molecular geometry already induces a qualitatively different crystal packing. Changing the M−N bond length by a few hundredths of an angström is therefore relevant. Even modest changes in molecular size or shape, which only induce slightly different intermolecular distances, have a drastically amplified effect on the lattice energy in these molecular salts due to the long range interactions.

Implications to crystal structure and polymorph prediction strategies are considerable, since either known molecular structures determined by XRD or gas phase structures optimised at various levels of theory are employed as input to the packing and search algorithms used. These results suggest that routine polymorph prediction may be more severely hampered by inaccuracies in molecular structures than by inadequacies in the empirical intermolecular potentials. The key to a successful structure prediction is therefore input of the most accurate molecular structures.

In this respect it cannot be stressed too strongly that molecular dimensions obtained by X-ray crystal structure analysis in general may be considerably in error unless corrected for the effect of libration. In extreme cases, like for spherical molecular ions such as hexafluorophosphate, the bond length errors due to this effect may exceed 0.1 Å. Of course, errors of such magnitude in the molecular shape and/or size matter when trying to predict the relative stability of polymorphs.

Furthermore, X-ray structures used for deriving inter- and intramolecular force fields should be carefully checked. Low temperature determination may be given a higher weighting factor, while structures that suffer from any kind of disorder should be excluded. In the generation of molecular structures for polymorph prediction even high level ab initio calculations may not be accurate enough. Certainly, the extreme sensitivity of the lattice energy to the molecular shape in such molecular salts tests the limits of current day intramolecular force fields. Even with molecules of very limited conformational flexibility, a balanced description of intra- and intermolecular interactions proves to be a difficult task. The situation gets still more difficult with more flexible molecules where a precise balance between intra- and intermolecular interactions is required.

Aside from the problems inherent in the accuracy of input molecular structures and force fields, the purely thermodynamic approach ignores the fact that the kinetics of crystal nucleation may be actually responsible for selecting those polymorphs that will be found experimentally. This will require a deeper understanding of molecular recognition and self-organisation in the polymolecular subcritical nuclei present in supersaturated solutions[56,57] and the effect of solvent−solute interactions on nucleation.[58] It is reassuring that the presented results give confidence that modern day intermolecular potentials should be accurate enough to realistically model nucleation kinetics for these organometallic compounds.

Experimental Section

Computational Methods

Crystal Structure Models: Two types of crystal models were constructed for each polymorph of $[M(bpy)_3](PF_6)_2$ (M = Ru, Ni, Zn) using different molecular structures. The EXPTL crystal model used the experimental structures as reported in the literature and the preceding paper,[1,21,22,25] but corrected for well-recognised inadequacies of X-ray determination by positioning the hydrogen atoms at a bond length of 1.09 Å. Secondly, in the CORR crystal model the P−F bond length was also corrected for the apparent shortening caused by librational motion of the almost spherical anion. Applying the PLATON package[59] the principal axes and eigenvalues of the molecular libration tensor ***L*** and of the translation tensor ***T*** were estimated together with components of a tensor ***S*** that allows for the quadratic correlation between librational and translational motion[60] from the atomic displacement parameters (ADPs or U_{ij} tensor components). Since the polymorphs of $[M(bpy)_3](PF_6)_2$ are affected to a different extent by static and dynamic disorder, this TLS analysis was applied instead to $LiPF_6$ for which a very precise structure determination has been reported in the literature.[34]

The hypothetical starting structure for β-$[Zn(bpy)_3](PF_6)_2$, which is inaccessible experimentally, was obtained by averaging the molecular parameters of $[Zn(bpy)_3]^{2+}$ as observed in γ-$[Zn(bpy)_3](PF_6)_2$ in D_3-symmetry and importing this molecular structure into the structure of the Ru−analogue.

Electrostatic Model: The MEPs of the complex anions and cations were represented by point charges positioned at the nucleus of the atoms. As most widely used, point charges were fitted to the quantum mechanically calculated MEP[61] employing the program POL.[62] The net charge was constrained using a Lagrange multiplicator and least-squares fits were performed for points given on a rectangular grid (0.2 Å spacing) in a 0.7 Å thick layer outside the van der Waals surface. For the cation, the charge of the well-buried central atom was fixed to its Hirshfeld partition value.[63] Symmetry-equivalent atoms were averaged. The partial charges listed in the supporting information (Tables S1 and S2) reproduce the MEPs quite well, as indicated by the low relative root-mean-square values (< 3% for cations and 5.1% for $[PF_6]^-$) for the fits and should be well suited to represent the electrostatic interactions. The MEPs were calculated applying the density functional code DMol.[53] Molecular geometries for the single-point calculations were taken from X-ray structures with H atoms recalculated at idealised positions (C−H = 1.09 Å) and no symmetry restrictions were applied. We used DNP basis sets with inner cores frozen, a FINE integration grid, and the Vosko, Wilk, Nusair[64] parametrization of the correlation energy in the homogenous electron gas. The local spin-density approximation was used in SCF iterations and gradient corrections were added in a pertubative approach using the functionals proposed by Perdew and Wang[65] and Becke[66] for the correlation and exchange, respectively. The same approach was used for the single point energy calculations given in Table 6.

Rigid Body Minimisations: Within the rigid-body approach, molecules were considered to be rigid. The lattice energy was expressed as being purely intermolecular, and was calculated as the sum of intermolecular coulombic, dispersion and repulsion interactions between individual atom sites.

Applying the code MPA[9] the starting crystal models were relaxed using the method of static lattice energy minimisation with periodic boundary condition, which calculates the structure corresponding to the nearest energy minimum[9][67−69] in the context of a given set of interatomic potentials. The crystal structure was specified by six unit cell constants, three molecular rotation angles, and three *xyz* coordinates specifying the molecular centre. The site symmetry of molecules consequently needs to be lowered to C_1. Parameters related by space group or symmetry are connected by constraints.

The program calculates first (gradient) and second (Hessian) derivatives with respect to the above-mentioned variables. To remove imaginary modes from the Hessian, the program automatically selects energy minimisation by the OREM (off-ridge eigenvector minimisation[70]) method. If the Hessian is positive definite the NR (Newton−Raphson) method is used.

For evaluation of the slowly converging electrostatic and dispersion terms, accelerated convergence techniques are applied,[71] while the repulsion term is summed in real space (cut-off 15 Å).

It is a well-known fact that the lattice energy of a polar crystal, where the unit cell has a non-zero dipole moment, depends in principle on the external shape of the crystal.[72] Consequently, the lattice energy of the polar γ-modification cannot be given precisely unless the form of the crystals is specified. However, the γ-structure displays only a very small dipole moment {(e.g. −0.8008 eÅ for $\gamma_{200}(1)$−[Ni(bpy)$_3$](PF$_6$)$_2$}. Using the correction term derived by Smith[73] with the assumption of a spherical crystal ($2\pi p^2/3V$, with p and V being the dipole moment and the volume of the unit cell) a minor correction of 0.26 kJ/mol would apply for the total lattice energy. Therefore, no correction was applied to the values given in the Tables.

Four popular sets of empirical intermolecular potentials, CFF91,[28] Williams,[29], UNI,[30] and MM3,[31] were tested. It should be mentioned that all but the MM3 set are lacking some parameters and needed to be supplemented with parameters from other sources. Also, MPA will not allow the use of explicit parameters for mixed interactions, but instead uses combination rules to deduce these. Further, the combination rules are restricted to the common terms, $A_{ij} = (A_iA_j)^{1/2}$, $B_{ij} = (B_iB_j)^{1/2}$, $C_{ij} = (C_i + C_j)/2$, more elaborate rules as implemented in the CFF91 force field could not be used. Explicit values and details are given in the supporting information (Table S3).

Flexible Body Minimizations: The parametrization was performed according to the new method developed by Norrby and Liljefors with simultaneous use of experimental and quantum mechanical data.[44,46−49] A slightly modified *penalty function*[51] from the one used for the MM3* parametrization[44] was applied. Inverse distances were utilised instead of bond and torsion angles. The weighting factors employed are given in the supporting information (Table S8). Starting with the MM3* values, the stretching, bending, and torsional parameters involving ruthenium were optimised by minimising the penalty function using numerical NR techniques.[47] The same mass-weighted Hessian elements and structural data applied in the previous derivation of the MM3* parameters were used in the fit. Starting values involving the coordinating N−atom types (np_x, np_y, np_z) were taken from the CFF91[28] force field (np). The subscript is needed in order to be able to differentiate between *cis* and *trans* configurations in the angle-bending term, otherwise the atom types are equivalent and they are abbreviated np_{xyz}. Furthermore, the original CFF91 force field contains no appropriate atom type for the pyridyl−pyridyl bridge (cpp). This new atom type was also included in the fitting procedure. The starting values were taken from the corresponding atom type for biphenyl as contained in CFF95 (cpb).[74]

Parameters for the anion $[PF_6]^-$ were derived in a consistent way. The geometry was fully optimised in O_h symmetry, whereupon the Hessian was calculated numerically. The mass-weighted Hessian elements were used in the parametrization. Calculations employed the Gaussian94[75] program. The B3LYP[76][77] hybrid functional was used together with the 6−31G* basis set. The quantum mechanically determined P−F distance in the gas phase is much longer (1.648 Å) than the experimentally observed value in the solid state. This was noted before[52] by others even with better basis sets and is not a shortcoming of the ab initio method, but is due to the lack of an embedding environment as anions are very sensitive to this. Ideally, a perfect force field should be able to reproduce the bond shortening that will occur upon incorporation of the anion into the crystal field. Since the force field failed to fully match this appreciable bond shortening when going into the solid state the problem was "fixed" by shifting the r_0 value derived in the fitting procedure to the *TLS* corrected value (1.61 Å). Since there are not enough reliable experimental values available for the anion only QM information could be utilised in the parametrization. In the fitting procedure the same partial charges were used as in the lattice minimisations.

Supporting information for this article (Tables S1 and S2 with partial charges, Table S3 with intermolecular potentials, Tables S4−S7 with the contributions to the total lattice energy, Table S8 with waiting factors used for the penalty function, and Tables S9−S13 with intramolecular potential parameters) is available on the WWW under http://www.wiley-vch.d/home/eurjic or from the corresponding author.

Acknowledgments

We would like to thank Prof. Dr. K. -J. Range for making equipment available and for miscellaneous support, the Fonds der Chemischen Industrie, and the DFG for financial support. Also, we are grateful to Professor Caroline Röhr for kindly providing the atomic coordinates and U_{ij} values for $LiPF_6$. Furthermore, we thank the Degussa AG for a donation of $RuCl_3 \cdot 3H_2O$.

[1] J. Breu, H. Domel, A. J. Stoll, *Eur. J. Inorg. Chem.* **2000**, 2401−2408, preceeding paper.
[2] M. Tremayne, P. Lightfoot, C. Glidewell, K. D. M. Harris, K. Shankland, C. J. Gilmore, G. Bricogne, P. G. Bruce, *J. Mater. Chem.* **1992**, *2*, 1301−1302.
[3] T. S. Bush, C. R. A. Catlow, P. D. Battle, *J. Mater. Chem.* **1995**, *5*, 1269−1272.
[4] B. M. Kariuki, H. Serrano-Gonzalez, R. L. Johnston, K. D. M. Harris, *Chem. Phys. Lett.* **1997**, *280*, 189−195.
[5] Y. G. Andreev, P. G. Bruce, *J. Chem. Soc., Dalton Trans.* **1998**, 4071−4080.
[6] H. R. Karfunkel, F. J. J. Leusen, R. J. Gdanitz, *J. Computer-Aided Mater. Design* **1993**, *1*, 177−185.
[7] A. Gavezzotti, G. Filippini, *J. Am. Chem. Soc.* **1996**, *118*, 7153−7157.
[8] A. M. Chaka, R. Zaniewski, W. Youngs, C. Tessier, G. Klopman, *Acta Cryst. B* **1996**, *52*, 165−183.
[9] D. E. Williams, *Acta Cryst. A* **1996**, *52*, 326−328.
[10] D. M. Hofmann, T. Lengauer, *J. Mol. Model.* **1998**, *4*, 132−144.
[11] W. T. M. Mooij, B. P. van Eijck, S. L. Price, P. Verwer, J. Kroon, *J. Comput. Chem.* **1998**, *19*, 459−474.
[12] B. P. van Eijck, J. Kroon, *J. Comput. Chem.* **1999**, *20*, 799−812.
[13] M. Jansen, J. C. Schön, *Z. Anorg. Allg. Chem.* **1998**, *624*, 533−540.
[14] R. J. Gdanitz, in *Theoretical Aspects and Computer Modeling*

of the Molecular Solid State (Ed.: A. Gavezzotti). John Wiley Sons, Chichester, **1997**.
[15] P. Verwer, F. J. J. Leusen, in *Reviews in Computational Chemistry* (Eds.: K. B. Lipkowitz, D. B. Boyd), Wiley-VCH, New York, **1998**.
[16] A. Gavezzotti, *Crystallography Reviews* **1998**, *7*, 5−121.
[17] A. Gavezzotti, G. Filippini, *J. Am. Chem. Soc.* **1995**, *117*, 12299−12305.
[18] R. S. Payne, R. C. Rowe, R. J. Roberts, M. H. Charlton, R. Docherty, *J. Comput. Chem.* **1999**, *20*, 262−273.
[19] J. D. Dunitz, in *The Crystal as a Supramolecular Entity* (Ed.: G. R. Desiraju), John Wiley & Sons Ltd., **1996**.
[20] S. Dick, *Z. Kristallogr. New Crystal Structures* **1998**, *213*, 356.
[21] D. P. Rillema, D. J. Jones, *J. Chem. Soc., Chem. Commun.* **1979**, 849−851.
[22] D. P. Rillema, D. S. Jones, C. Woods, H. A. Levy, *Inorg. Chem.* **1992**, *31*, 2935−2938.
[23] E. C. Constable, P. R. Raithby, D. N. Smit, *Polyhedron* **1989**, *8*, 367−369.
[24] M. M. Richter, B. Scott, K. J. Brewer, R. D. Willett, *Acta Cryst. C* **1991**, *47*, 2443−2444.
[25] M. Biner, H.-B. Bürgi, A. Ludi, C. Rohr, *J. Am. Chem. Soc.* **1992**, *114*, 5197−5203.
[26] J. Breu, C. Kratzer, H. Yersin, *J. Am. Chem. Soc.* **2000**, *122,* 2548−2555.
[27] J. Bernstein, R. J. Davey, J.-O. Henck, *Angew. Chem.* **1999**, *111*, 3646−3669; *Angew. Chem. Int. Ed.* **1999**, *38*, 3440−3461.
[28] CFF91 force field. Molecular Simulation. (December 1991): 9658 Scranton Road, San Diego, CA 92121−2777, USA: MSI. (1991).
[29] D. E. Williams, D. J. Houpt, *Acta Cryst. B* **1986**, *42*, 286−295.
[30] G. Filippini, A. Gavezzotti, *Acta Cryst. B* **1993**, *49*, 868−880.
[31] N. L. Allinger, X. Zhou, J. Bergsma, *J. Mol. Struc.* **1994**, *312*, 69−83.
[32] J. D. Gale, *Phil. Mag. B* **1996**, *73*, 3−19.
[33] D. W. J. Cruickshank, *Acta Cryst.* **1956**, *9*, 754−756.
[34] C. Röhr, R. Kniep, *Z. Naturforsch. (B)* **1994**, *49*, 650−654.
[35] C. B. Aakeröy, M. Nieuwenhuyzen, S. L. Price, *J. Am. Chem. Soc.* **1998**, *120*, 8986−8993.
[36] T. Liljefors, I. Petterssen, *J. Comput. Chem.* **1987**, *8*, 1139−1145.
[37] W. L. Jorgensen, D. L. Severance, *J. Am. Chem. Soc.* **1990**, *112*, 4768−4774.
[38] C. A. Hunter, in *From Simplicity to Complexity in Chemistry − and beyond* (Ed.: A. Müller), Vieweg, Braunschweig, **1996**.
[39] I. Dance, M. Scudder, *J. Chem. Soc., Dalton Trans.* **1998**, 1341−1350.
[40] C. S. Wilcox, E. Kim, S. Paliwal, *J. Am. Chem. Soc.* **1998**, *120*, 11192−11193.
[41] C. S. Wilcox, S. Paliwal, S. Geib, *J. Am. Chem. Soc.* **1994**, *116*, 4497−4498.
[42] D. Buttar, M. H. Charlton, R. Docherty, J. Starbuck, *J. Chem. Soc., Perkin Trans. 2* **1998**, 763−772.
[43] J. Starbuck, R. Docherty, M. H. Charlton, D. Buttar, *J. Chem. Soc., Perkin Trans. 2* **1999**, 677−691.
[44] P. Brandt, T. Norrby, B. Åkermark, P.-O. Norrby, *Inorg. Chem.* **1998**, *37*, 4120−4127.
[45] Cerius-OFF. Molecular Simulation. (2 3.5): 9658 Scranton Road, San Diego, CA 92121−2777, USA: MSI. (1996).
[46] P.-O. Norrby, P. Brandt, *Coord. Chem. Rev.* **2000**, in print.
[47] P.-O. Norrby, T. Liljefors, *J. Comput. Chem.* **1998**, *19*, 1146−1166.
[48] P.-O. Norrby, T. Rasmussen, J. Haller, T. Strassner, K. N. Houk, *J. Am. Chem. Soc.* **1999**, *121*, 10186−10192.
[49] P.-O. Norrby, in *Computational Organometallic Chemistry* (Ed.: T. Cundari), Marcel Dekker, New York, **2000**.
[50] U. Burkert, N. L. Allinger, *Molecular Mechanics*, American Chemical Society, **1982**.
[51] C. Breen, J. S. Brooks, S. Forder, J. C. E. Hamer, *J. Mater. Chem.* **1996**, *6*, 849−859.
[52] B. I. Robinson, S. A. Johnson, T. H. Tang, R. J. Gillespie, *Inorg. Chem. 36,* **1997**, *14*, 3022−3030.
[53] B. Delley, *J. Chem. Phys.* **1990**, *92*, 508−517.
[54] G. R. Parr, W. Yang, in *Density-Functional Theory of Atoms and Molecules*, Oxford University Press, Oxford, **1989**.
[55] R. J. Boyd, J. Wang, in *Recent Advances in Density Functional Methods* (Ed.: D. P. Chong), World Scientific, Singapore, **1995**.
[56] A. Gavezzotti, G. Filippini, *J. Chem. Soc.,Chem. Commun.* **1998**, 287−294.
[57] A. Gavezzotti, *Chem. Eur. J.* **1999**, *5*, 567−576.
[58] N. Bladgen, R. J. Davey, H. F. Liebermann, L. Williams, R. Payne, R. Roberts, R. Rowe, R. Docherty, *J. Chem. Soc., Faraday Trans.* **1998**, *94*, 1035−1044.
[59] A. L. Spek, *Acta Cryst. A* **1990**, *46*, C34.
[60] V. Schomaker, K. N. Trueblood, *Acta Cryst. B* **1968**, *24*, 63−76.
[61] E. Sigfridsson, U. Ryde, *J. Comput. Chem.* **1998**, *19*, 377−395.
[62] POL − Program for Derivation of Molecular Electrostatic Properties from DMOL DFT Calculations. Grochowski,P. Warsaw University: (**1995**).
[63] F. L. Hirshfeld, *Theoret. Chim. Acta* **1977**, *44*, 129−138.
[64] S. H. Vosko, L. Wilk, M. Nusair, *Can. J. Phys.* **1980**, *58*, 1200−1211.
[65] J. P. Perdew, Y. Wang, *Phys. Rev. B* **1992**, *45*, 13244−13249.
[66] A. D. Becke, *J. Chem. Phys.* **1988**, *88*, 2547−2553.
[67] J. D. Gale, *J. Chem. Soc., Faraday Trans.* **1997**, *93*, 629−637.
[68] C. R. A. Catlow, L. Ackermann, R. G. Bell, F. Cora, D. H. Gay, M. A. Nygren, J. C. Pereira, G. Sastre, B. Slater, P. E. Sinclair, *Faraday Discuss.* **1997**, 1−40.
[69] G. W. Watson, P. Tschaufeser, A. Wall, R. A. Jackson, S. C. Parker, in *Computer Modelling in Inorganic Crystallography* (Ed.: C. R. A. Catlow), Academic Press Inc., San Diego, **1997**.
[70] D. E. Williams, *Chem. Phys. Lett.* **1992**, *192*, 538−543.
[71] D. E. Williams, in *International Tables for Crystallography, Vol. B, Reciprocal Space* (Ed.: U. Shmueli) Kluwer Academic Publishers, Dordrecht, **1993**.
[72] B. P. van Eijck, J. Kroon, *J. Phys. Chem. B* **1997**, *101*, 1096−1100.
[73] E. R. Smith, *Proc. Royal Soc. A* **1981**, *375*, 475−505.
[74] CFF95 force field. Molecular Simulation. (December 1998): 9658 Scranton Road, San Diego, CA 92121−2777, USA: MSI. (1995).
[75] M. J. Frisch, G. W. Trucks, H. B. Schlegel, P. M. W. Gill, P. G. Johnson, M. A. Robb, J. R. Cheesemen, T. A. Keith, J. A. Petersson, J. A. Montgomery, K. Raghavachari, L. A. Al-Laham, V. G. Zakrzewski, J. V. Ortiz, J. B. Foresman, J. Cioslowski, B. B. Stefanov, A. Nanayakkara, M. Challacombe, C. Y. Peng, P. Y. Ayala, W. Chen, M. W. Wong, J. L. Andres, E. S. Replogle, R. Gomperts, R. L. Martin, D. J. Fox, J. S. Binkley, D. J. DeFrees, J. Baker, J. J. P. Stewart, M. Head-Gordon, C. Gonzales, J. A. Pople, *Gaussian 94*, Gaussian, Inc., Pittsburgh, PA, **1995**.
[76] C. Lee, W. Yang, R. G. Parr, *Phys. Rev. B* **1988**, *37*, 785−789.
[77] A. D. Becke, *J. Chem. Phys.* **1993**, *98*, 5648−5652.
[78] D. E. Williams, *Acta Cryst. A* **1972**, *28*, 84−88.
[79] N. L. Allinger, J. H. Yuh, J. H. Lii, *J. Am. Chem. Soc.* **1989**, *111*, 8551−8566.
[80] S. L. Mayo, B. D. Olafson, W. A. Goddard, *J. Phys. Chem.* **1990**, *94*, 8897−8909.

Received February 8, 2000
[I00043]